

Using Fourier Analysis of Spiral Density Waves to Unravel Saturn's Interior Dynamics

A Project submitted in Partial Fulfilment for the requirement of MATH537 (Fourier Analysis)

Victor Afigbo

University of Idaho, Moscow Campus

Spring (April) 2023

Abstract

Saturn's rings exhibit complex dynamics, including spiral density waves, which are spiral patterns that propagate through the ring system. These waves are generated by gravitational perturbations from nearby moons and can provide important information about the structure and dynamics of the rings. In recent years, astronomers have focused on studying these spiral density waves to better understand their formation and evolution. In this project, we explore the role of Saturn's interior dynamics in shaping its rings by analyzing the amplitude of spiral density waves, using efficient Fourier transformation algorithms, and investigating the characteristics of these waves. We present the relevant Fourier transformation equations and apply them to data from the Cassini spacecraft to determine the properties of the spiral density waves in Saturn's C ring. Our findings, using the efficient algorithms, suggest that the waves are strongly influenced by Saturn's internal structure, including its rotation rate and density distribution. Our analysis also reveals previously unknown information about the properties of these waves, including their wavelength and frequency, which can help us further understand the underlying physics of Saturn's rings, as well as Saturn's interior dynamics. These results have important implications for our understanding of the formation and evolution of planetary ring systems and may shed light on the processes that led to the formation of our own Solar System.

1 Introduction

Saturn's rings are a fascinating and complex system of particles that exhibit a wide range of phenomena. These phenomena include density waves, shepherding moons, and the Cassini division, among others. Density waves are particularly interesting because they represent a mechanism by which the rings can exchange angular momentum with each other and with Saturn's moons. Spiral density waves are a special type of density wave that arise from the interaction between the rings and a perturbing moon. These waves have been observed in several locations in the ring system, including the A, B, and C rings. The amplitude of spiral density waves is an important parameter that can provide insights into the underlying physics of the system. Fourier transforms, on the other hand, are a powerful tool for analyzing periodic phenomena such as these waves, and are widely used in signal processing and data analysis. By decomposing the signal into its constituent frequencies, we can gain insights into the amplitude, phase, and wavelength of the waves. In this project, we will apply Fourier transforms to data from the Cassini spacecraft to investigate the characteristics of the spiral density waves in different locations in Saturn's rings.

The understanding of Saturn's rings has developed since their discovery by Galileo Galilei in 1610 [2]. Huygens recognized that the rings are a disk in 1656, and with each advance in observations, new structures have been revealed [2][4][7]. The rings have distinct characteristics on different scales, and moons play a crucial role in shaping their structure. The A and B rings' outer edges are shepherded and sculpted by resonances with co-orbitals and Mimas, respectively, and the majority of large-scale features in the A ring are caused by density waves at the locations of orbital resonances with nearby and embedded moons. The C ring's strategic location with respect to Saturn's gravitational perturbations is a topic of interest, leading to unique and dynamic features.

1.1 Saturn's C Ring

Saturn's C ring is one of the most fascinating features of the sixth planet from the sun, spanning from about 74,658 km to 92,000 km from the planet's center, lying between the brighter B ring and the more diffuse D ring. The C Ring is made up of small particles ranging in size from micrometers to centimeters, and it is unique in that it has a peculiar wave-like pattern [2][8][12]. The waves across the C Ring were first observed by the Voyager spacecraft in the early 1980s. These waves are

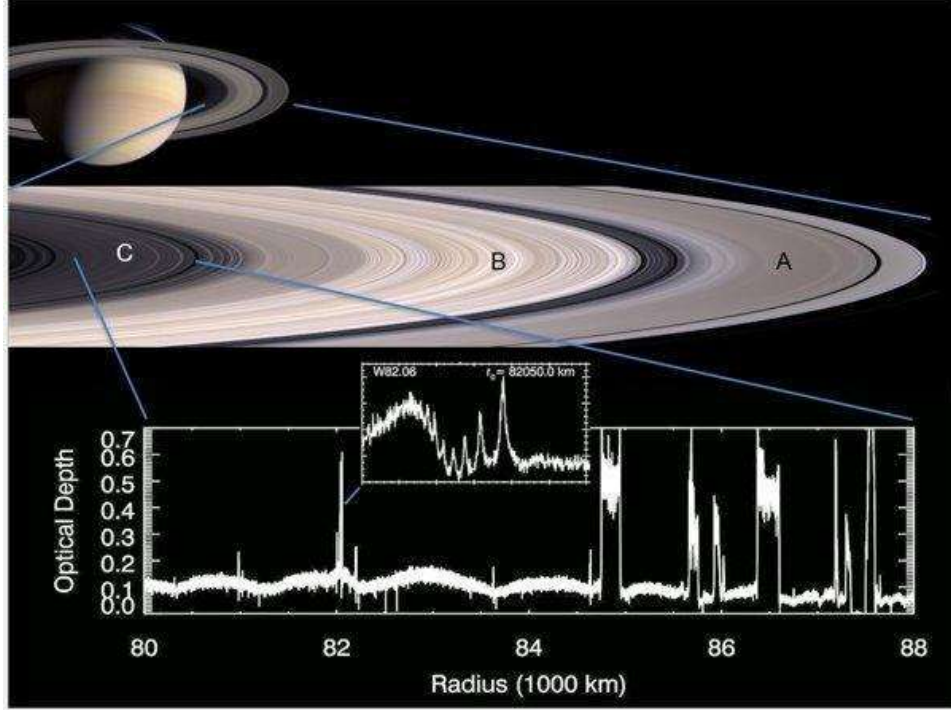


Figure 1: A picture of the A, B and C(Zoomed in) rings [8]. An optical depth profile zoomed in on one of the waves (W82.06).

caused by gravitational interactions between the ring particles and Saturn's moons. As the moons pass by the ring, they create a gravitational disturbance that propagates through the ring in the form of a wave[6][7][8][10][12]. These waves in the C Ring are incredibly precise, with wavelengths ranging from 30 to 180 kilometers. They are also very consistent, with the same patterns appearing year after year. The cause of this consistency is still not fully understood, but it is believed to be related to the structure of the ring particles themselves [6][7][8].

1.2 Density Waves

Spiral density and bending waves are well-researched and understood phenomena in the rings of Saturn, and they have provided valuable information about the surface mass density and viscosity of the main ring regions [2][6][9]. The majority of these waves are caused by resonances with external satellites, especially in the A and B rings. However, another set of waves has been discovered in recent times, primarily in the C ring, which are not caused by satellites but by irregularities in Saturn's own gravitational field [6][7][8]. Our focus is on studying the waves that are generated in Saturn's rings by the planetary normal modes. Specifically, we are exploring the inner C ring which has not been extensively researched before [4][6]. The waves in this area have very short wavelengths, which has posed a challenge for previous studies as they relied on precise calculations of wave phases to identify them [4][6][8][15]. In the next section, we aim to outline the basics of Fourier analysis and device an efficient algorithm for Fourier transformations, to use in processing Cassini's VIMS (Visual and Infrared Mapping Spectrograph) data, since other tested algorithms have resulted to an inefficient result. Thereafter, we will apply the new algorithm to our data and present the results achieved using this technique.

2 Theory

2.1 Spiral Density Waves

In this section, we outline the concept of spiral density waves, how it is formed across Saturn's C ring and the mathematical representation of such phenomenon. Basically, when normal-mode oscillations take place within gaseous planets, like Saturn, they do so in terms of vibrations, and these vibrations in turn give rise to variations in density within the planet, causing disturbances to be generated within the planet, and these disturbances in turn propagate towards the exterior of Saturn. Saturn's gravitational field simply couples these disturbances to the plane of the rings, and these disturbances travel across the stretch of the ring in form of density waves, spiral density and spiral bending waves. Our main focus is on the spiral density waves since their main cause are as a result of normal mode excitation within Saturn.

2.1.1 Linear Density Wave Model

For a better understanding of the applications of Fourier transforms on the spiral density wave analysis, we need to outline the theory behind the algorithms used in the subsequent section. Here, we are utilizing the density wave model to produce anticipated wave profiles [12]. The specific model we are using is the linear, damped model which was originally derived and elaborately introduced by Shu in 1984 [5]. To provide the essential details for our project, we will give a concise explanation of the model equations as well as the model parameters. This will help us to understand the workings of the model better and enable us to use it more effectively in our project. The linear, damped model is a well-established method that has been utilized in many scientific studies to describe a variety of astronomical phenomena.

Usually, when these waves are propagated across the ring, they are displayed as fluctuations in the density of the ring's surface, which affects its optical properties. This fluctuation has an m-fold symmetry and rotates with respect to the fixed reference frame at a rate of Ω_p . The altered surface density distribution, normalized to the background density in areas outside the waves' region, Σ , is represented by the expression:

$$\frac{\sigma(r, \lambda, t)}{\Sigma} = A_L \xi e^{-\left(\frac{\xi}{\xi_D}\right)^3} \cos \left[\phi - \frac{3\pi}{4} - \xi^2 \right] \quad (1)$$

Here, $\sigma(r, \lambda, t)$ is the perturbed surface density distribution of the ring section, r is the distance (in kilometers) away from the center of the planet, λ and t are the longitude and time of observation, respectively. A_L is the dimensionless amplitude factor, $\phi = m(\lambda_s(0) + \Omega_s t - \lambda)$ is the wave phase; $\lambda_s(0)$ is the mean longitude of the satellite at $t = 0$ and Ω_s is the orbital mean motion of the satellite. ξ_D is the dimensionless damping length. From [12], ξ is a dimensionless quantity that specifies the distance from the resonant radius, r_L , and it is given as:

$$\xi = \left[\frac{3(m-1)\Omega_L^2 r_L}{4\pi \Sigma G} \right]^{\frac{1}{2}} \left(\frac{r - r_L}{r_L} \right) \quad (2)$$

G is the Newtonian gravitational constant equivalent, in SI units, to $6.674 \times 10^{-11} m^3 kg^{-1} s^{-2}$.

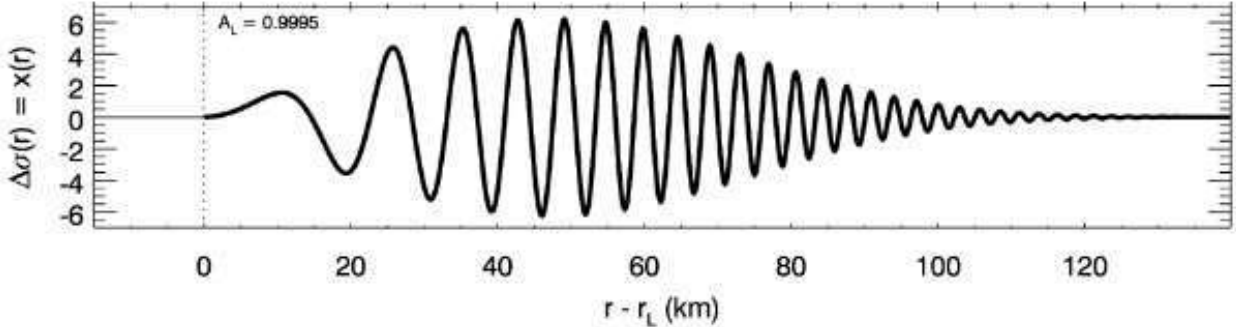


Figure 2: Synthetic density-wave radial profile generated by Equation (1) [15].

2.2 Wavelet Analysis

Now that we have laid out the fundamental theoretical groundwork for spiral density waves, our next objective is to build the mathematical tools needed to apply Fourier transform. These tools are essential for enabling a more accurate and rigorous analysis of the intricate dynamics of spiral density waves, including their periodic patterns and frequencies. Moreover, Fourier transform will provide us with valuable insights into the underlying physical properties of these waves, which will be essential for understanding their behavior and predicting their future evolution. Ultimately, our application and interpretation of Fourier transform algorithms will help to shed light on the complex nature of spiral density waves and how they are excited from Saturn's interior. Wavelet analysis is a method of time-frequency analysis that is scale independent and can provide more detailed information about the dominant frequencies present in a signal than traditional Fourier analysis. This is because wavelets can adapt to the local features of the signal at different scales, allowing for a more accurate representation of the signal's frequency content. In contrast, traditional Fourier analysis assumes a fixed window size, which can lead to inaccuracies in the frequency estimation of signals with non-stationary or time-varying properties. Thus, for signals with a wide range of dominant frequencies or non-stationary properties, wavelet analysis is often a more appropriate method of analysis [16].

2.3 Continous Wavelet Transform

Assuming our unprocessed signal is given as $x(t)$. From [11][13], we use a normalized wavelet $\psi \in L^2(\mathbb{R})$, having zero average, with shifting and rescaling parameters b and a , respectively:

$$\psi_{a,b}(t) = \frac{1}{\sqrt{|a|}} \psi\left(\frac{t-b}{a}\right) \quad (3)$$

The Continous Wavelet Transformation derivable from our signal, $x(t)$, is given as:

$$X_w(a, b) = \langle x, \psi_{a,b} \rangle = \int_{-\infty}^{+\infty} x(t) \psi_{a,b}^*(t) dt \quad (4)$$

Here, $\psi_{a,b}^*(t)$ is the complex conjugate of $\psi_{a,b}(t)$. We can rewrite equation 4 as: $X_w(a, b) = \frac{1}{\sqrt{|a|}} \int_{-\infty}^{+\infty} x(t) \bar{\psi}\left(\frac{t-b}{a}\right) dt$ and let $\tilde{X}_w(a, b) = \int_{-\infty}^{+\infty} x(t) \bar{\psi}\left(\frac{t-b}{a}\right) dt$. Then our new equation 4 becomes: $X_w(a, b) = \frac{1}{\sqrt{|a|}} \tilde{X}_w(a, b)$. Here, the prefactor $\frac{1}{\sqrt{|a|}}$ is introduced in order to ensure that all scaled functions with $a \in \mathbb{R}$ have the same energy [11][14][16]. Note also that $b \in \mathbb{R}$.

2.4 Wavelet Reconstruction Formula

For proper reconstruction, and assuming $x \in L^2(\mathbb{R})$, we can reconstruct our signal using the famous Calderon's technique [1][13][14][16]:

$$x(t) = \frac{1}{C_\psi} \int_0^\infty \int_{-\infty}^\infty X_w(a, b) \frac{1}{|a|^{1/2}} \psi\left(\frac{t-b}{a}\right) \frac{db da}{a^2}, \quad (5)$$

provided $\psi(t)$ satisfies Calderón's admissibility condition [1]: $C_\psi := \int_{-\infty}^\infty \frac{|\tilde{\psi}(\xi)|^2}{|\xi|} d\xi < \infty$ and must have a finite energy[14][16]: $E_\psi = \int_{-\infty}^\infty |\psi(t)|^2 dt < \infty$. Here, $\tilde{\psi}(\omega)$ is the Fourier transform of $\psi(t)$, $\omega = 2\pi f$ is the angular frequency, and C_ψ is the admissibility constant. The above condition implies that $\tilde{\psi}(\omega)$ approaches zero faster than ω and must not have zero frequency component, $\tilde{\psi}(0) = 0$ [14].

2.4.1 Choice of Wavelet Function

An efficient example of a wavelet function that is “admissible”, has zero mean and is localized in both time and frequency space, is the Morlet wavelet[3][11][16]. It consists of a plane wave modulated by a Gaussian[16]:

$$\psi(t) = \pi^{-1/4} e^{i\omega_0 t} e^{-t^2/2} \quad (6)$$

where $\omega_0 = 6$, a dimensionless frequency which satisfies the admissibility condition [3][11][16].

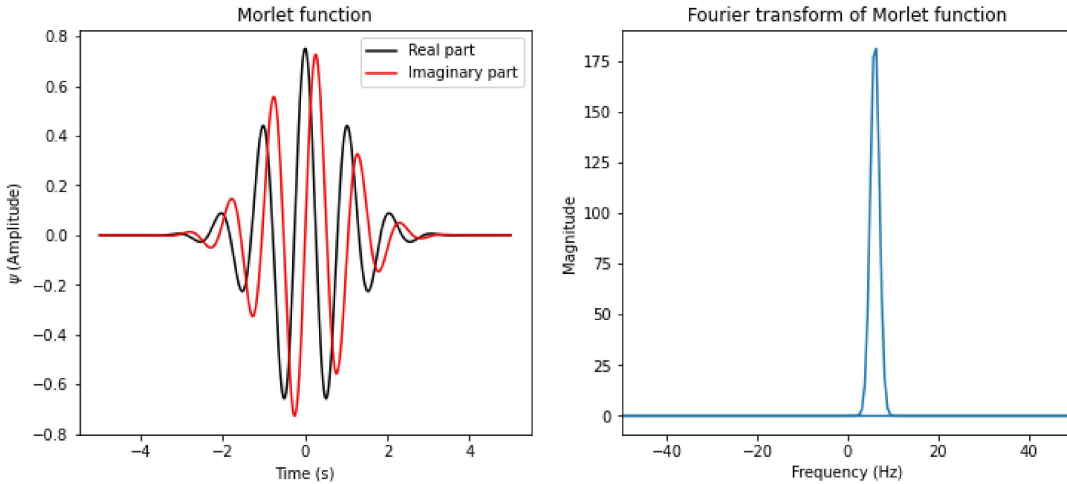


Figure 3: Morlet function in time (real and imaginary) and frequency space.

It is worthy of note that, the Morlet wavelet does not have compact support but has exponential decay. This means that the wavelet function does not go to zero outside a certain range of values, but instead decays exponentially. Regarding the differentiability of the Morlet wavelet, it is not infinitely differentiable. No wavelet with finite support can be infinitely

differentiable. This is because, for a wavelet to have compact support, it must be zero outside a certain interval. However, if a function is zero outside an interval, then it cannot have nonzero derivatives of all orders.

Finally, the Morlet wavelet does not come from an MRA (multiresolution analysis). This means that the Morlet wavelet cannot be generated by a series of dilations and translations of a single wavelet function, which is a key feature of MRAs. However, the Morlet wavelet can still be used in wavelet analysis for certain applications, like in our case.

2.5 Alternative Wavelet function

Recall, $X_w(a, b) = \frac{1}{\sqrt{|a|}} \tilde{X}_w(a, b)$. By direct substitution into equation 5, we have:

$$x(t) = \frac{1}{C_\psi} \int_0^\infty \int_{-\infty}^\infty \frac{\tilde{X}_w(a, b)}{|a|} \psi\left(\frac{t-b}{a}\right) \frac{db da}{a^2}. \quad (7)$$

We can also choose a completely different wavelet function, Morlet's technique, like the Dirac-delta function $\delta\left(\frac{b-t}{a}\right)$, instead of the analysing wavelet [3][14]. Here:

$$x(t) = \frac{1}{C_\psi} \int_0^\infty \frac{1}{|a|} \left(\int_{-\infty}^\infty \tilde{X}_w(a, b) \delta\left(\frac{t-b}{a}\right) db \right) \frac{da}{a^2} \quad (8)$$

Recall for a Delta function, $\delta(-x) = \delta(x)$ and $\int_{-\infty}^\infty \delta(x-d) f(x) dx = f(d)$.

Using $b = ay$, and working through the double-integral, we have: $\int_{-\infty}^\infty \tilde{X}_w(a, b) \delta\left(\frac{t-b}{a}\right) db = a \tilde{X}_w(a, t)$.

By direct substitution into equation 5, we arrive at a simplified single integral for our wavelet reconstruction given as [3][14][16]:

$$x(t) = \frac{1}{C_\delta} \int_0^\infty \frac{\tilde{X}_w(a, t)}{|a|} \frac{da}{a}. \quad (9)$$

Note: $C_\psi = C_\delta$, since we reconstructed the Fourier transforms using a Dirac delta function [16].

2.6 Choice of Scale: From Dyadic to Linear Scale

Since we are working with nonorthogonal wavelet analysis, it is recommendable to use an arbitrary set of scale to build a more complete wavelet reconstruction for equation 9 above [16]. To enable us succeed in this case, we assume a variant of the dyadic scales given in [13][16]:

$$a_j = a_0 2^{j\delta_j} \quad (10)$$

where, $j = 0, 1, 2, \dots, J$; a_0 is the smallest resolvable scale, assumed to be constant for our data. δ_j is the scaled range of wavelength measurement, with respect to the non-dimensional frequency, ω_0 , given as:

$$\delta_j = \tilde{\epsilon} \Delta a, \quad (11)$$

Here, $\tilde{\epsilon} = \sup\{\phi \in \mathbb{R} : 0 < \phi \leq \omega_0\}$ and $\Delta a = [a(j), a(j+1)]$, assumed to be constant for our specific signal data.

First, to linearize the dyadic scale, we take the natural logarithm of equation 10: $\ln a_j = \ln a_0 + j\delta_j \ln 2$. Now, differentiating the previous equation with respect to j simply produces the result: $\frac{da_j}{a_j} = \delta_j \ln 2$. Note here that, $dj = (j+1) - j = 1$ for discrete case. Finally, we substitute the result of the latest differential equation into the equation 9, and express the total results discretely, in the following steps.

Substituting the constants and variables into equation 9, we have:

$$x(t) = \frac{\tilde{\epsilon} \Delta a \ln 2}{C_\delta} \sum_{j=0}^J \frac{\tilde{X}_w(a_j, t)}{|a_j|} \quad (12)$$

Practically, our reconstructed time series can be taken as the sum of the real part of the wavelet transform over all scales [16]. Taking the approximation of the aforesaid reconstruction, our final result becomes:

$$x_\alpha(t) = \tilde{\epsilon} \Delta a |\alpha| \sum_{j=0}^J \frac{\Re(\tilde{X}_w(a_j, t))}{|a_j|} \quad (13)$$

where $\alpha = \frac{\ln 2}{C_\delta \psi(0)}$, $C_\delta = 0.776$ [16]; $\psi(0) = \pi^{-1/4}$ [16]. $x_\alpha(t)$ is the final reconstructed form of $x(t)$. We will use this expression in our Python computational analysis in the section below.

2.7 Sample Reconstruction

In a bid to verify the authenticity of our customized wavelet reconstruction formula, we assume a noisy signal given by the equation:

$$x(t) = 5 \sin\left(2\pi\left(\frac{t}{0.02}\right) + 10\right) + 3 \sin\left(2\pi\left(\frac{t}{0.05}\right)\right) \quad (14)$$

where $t = \text{np.linspace}(0, 1, \text{nrx}=1000)$ in Python computations, $\Delta a = 1$, $\tilde{\epsilon} = \phi = 6.0$ and other constants having the same value as defined previously. We are going to compare our plot with that obtained using the PyWavelet Python library, below.

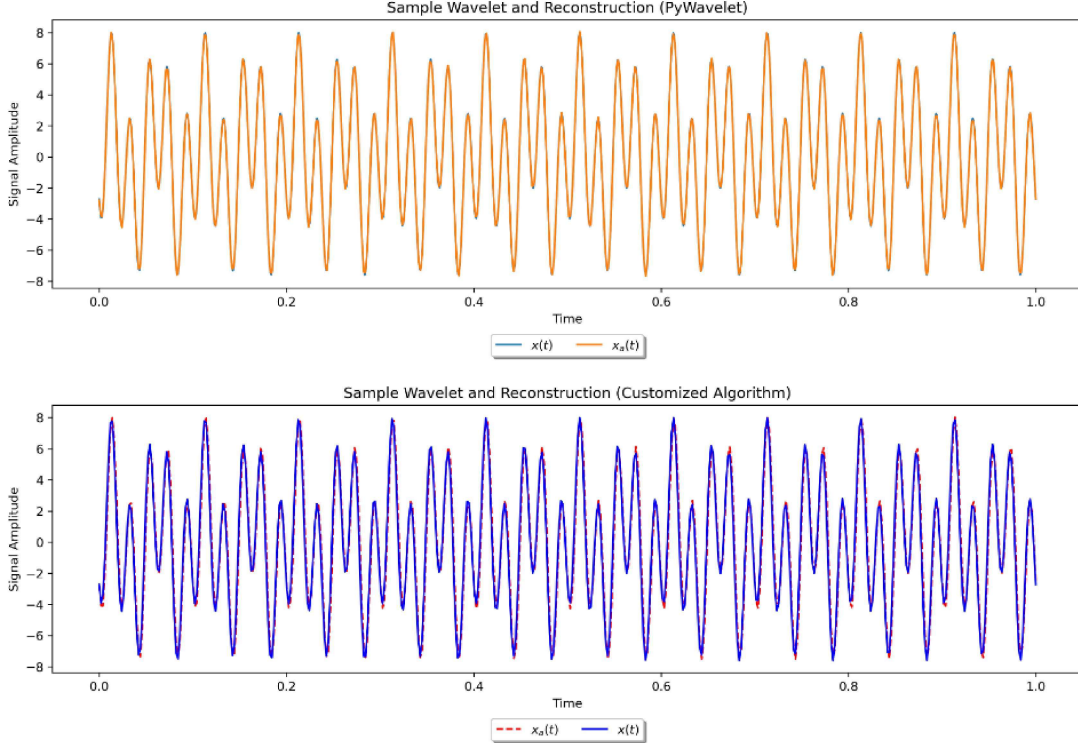


Figure 4: Sample Wavelet Plots (Main and Reconstructed Signals)

Method	Correction Factor	Flexibility
Customized Algorithm	1.0130	High
PyWavelet Package	1.0155	Limited
Scipy.signal Package	—	No Algorithm

Table 1: Comparison of correction factor and flexibility between different methods (Figure 5).

From the plots and table, the customized algorithm has the lowest correction factor and a high flexibility in terms of varying the parameters for accurate results. This factor represents how much the wavelet transform has modified the original signal in terms of relative magnitude. Specifically, a factor greater than 1 means that the modified signal has larger amplitude than the original signal, while a factor less than 1 means that the modified signal has smaller amplitude than the original signal. The Scipy.signal library has no documented wavelet reconstruction algorithm. The next section discusses the main results of using our customized codes on real wavelet data from the recent Cassini missions (2004 to 2017).

3 Implementation Routine

3.1 Data acquisition

To analyze the amplitude of spiral density waves in Saturn's C ring, we will first need to obtain VIMS(Visual and Infrared Mapping Spectrometer) data on the C ring structure. We can then use Fourier analysis to break down the ring structure in terms of its individual frequency (wavelength) components. Specifically, we will use data from the Cassini spacecraft, which

orbited Saturn from 2004 to 2017, to obtain measurements of the density waves in the rings. The data consists of images of the rings taken by the spacecraft.

3.2 Image processing

To apply Fourier transforms to the spiral density waves in Saturn's rings, we will first need to convert the set of images of the visual infrared and mapping spectrograph occultations for the ring structure, into a set of brightness values with higher values corresponding to regions of higher particle density, and vice-versa. The processed images contain information about the density waves, such as the location and shape of the waves in the images, as well as their amplitudes.

3.3 Fourier transform

We will first use the Continuous Wavelet Transform (CWT) algorithm to transform the time series of the amplitude measurements into the frequency domain. This will allow us to also perform phase correction of the distorted signals, owing to blockage or distortion by the planetary body.

3.3.1 Phase-Correction Algorithm In Fourier Space

In general, phase-correction is commonly used in signal processing to correct for phase distortions or misalignments that may have occurred during data acquisition or processing. In the context of planetary science or planetary seismology, phase correction may be used to correct for phase shifts or time delays in seismic signals caused by the propagation of seismic waves through a planetary body with a complex internal structure, like Saturn. For example, in the case of an occultation geometry, where a spacecraft passes behind a planet or moon and its signal is blocked or distorted by the planetary body, the seismic signals received by the spacecraft may be affected by the planet's internal structure, which can introduce phase shifts or time delays. By applying phase correction to the wavelet transform of the seismic signal, it may be possible to remove or mitigate some of these phase shifts or time delays, allowing for more accurate analysis and interpretation of the seismic data.

3.4 Signal Reconstruction

Here, we average the resulting signals present in the whole wave occultation, after the phase-corrected has been performed. We will utilize our customized algorithm in Python computing language to recover our signals.

4 Results

With the aid of the theoretical groundwork, coupled with the steps in the methodology, we implement the required algorithms in Python computing language and come up with the following plots shown below (Figure 6). Note, again, that the phase-correction algorithm applies phase shifts to the wavelet transform and then computes the average phase-corrected wavelets for each pattern speed.

The use of efficient algorithms has led to significant findings regarding the behavior of waves in Saturn's rings. In particular, the wave analysed has proven to be strongly impacted by the planet's internal structure, including its rotation rate and density distribution, and not by any of Saturn's moons [4][8]. The study also discovered new information about the properties of these waves, such as the slightly changing positions of their amplitudes. Further exploration of these information will enhance our understanding of the physics of Saturn's rings and the dynamics of the planet's interior, and contribute to our understanding of the composition and behavior of Saturn as well as its implications for other planets in our solar system.

5 Future Directions

There is still much to learn about spiral density waves in Saturn's rings, and efficient algorithms for Fourier transforms are an important tool for their analysis. One promising direction for future research is the use of Fourier transforms to study the interaction between spiral waves and other phenomena in the rings, such as resonances with nearby moons. Additionally, new data from the Cassini spacecraft and future missions to Saturn could provide even more detailed information about the structure and dynamics of the rings, opening up new avenues for analysis. To help achieve these objectives, we plan to achieve a more efficient correction factor for our customized algorithm, to help produce efficient and effective results during usage.

6 Conclusion

In conclusion, our study has shed new light on the behavior of waves within Saturn's rings and the factors that influence them. By using efficient Fourier transform algorithms, we were able to quantify the impact of the planet's internal structure

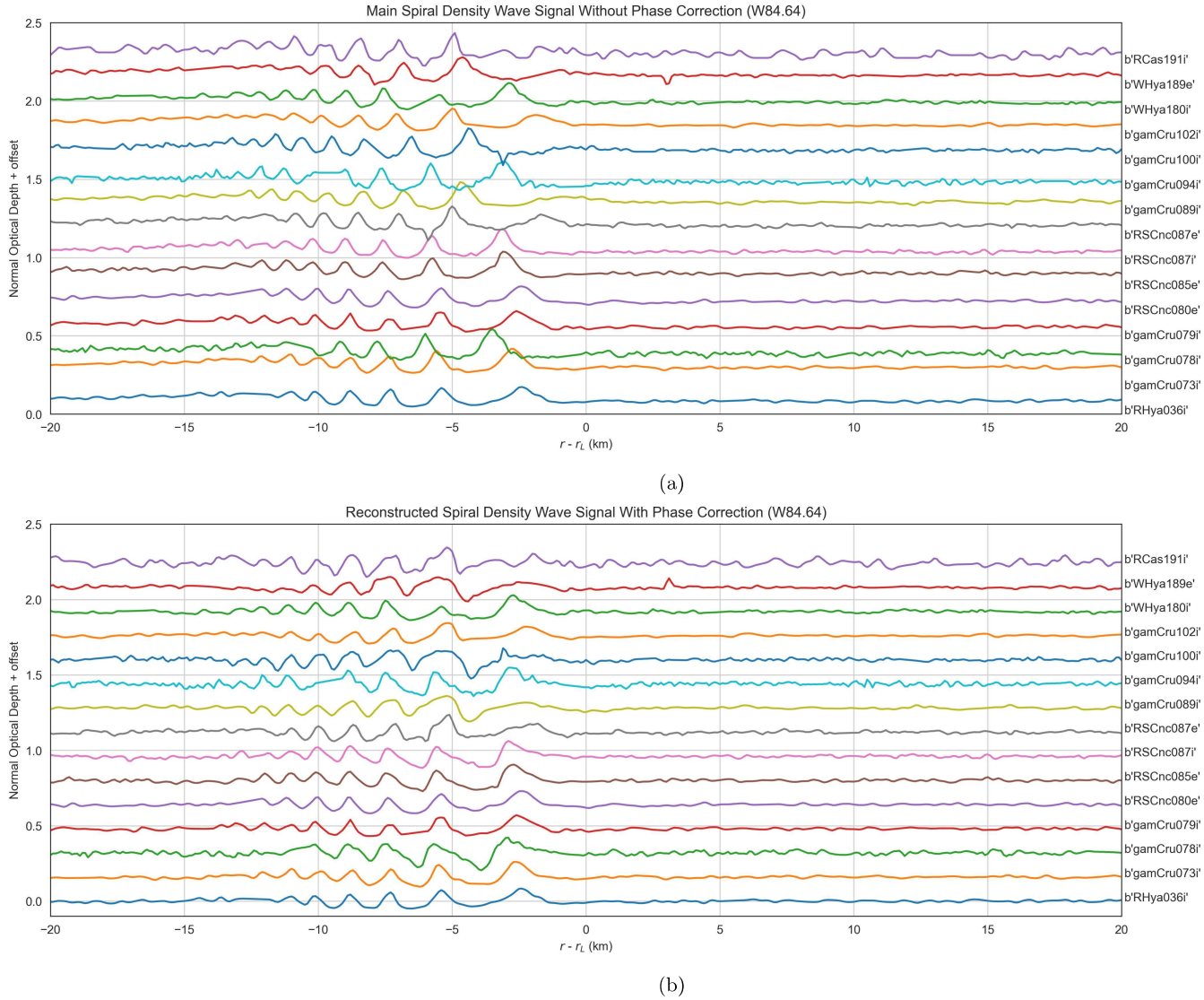


Figure 5: (a) A Plot of the Normal Optical depth (with vertical offset) for the wave profile (without phase correction). These wave profiles are noisy and not properly aligned. (b) A plot of the Normal Optical depth (with vertical offset) for the wave profile (with phase correction). Here, the profiles shown are not noisy and they mostly align properly.

on the behavior of these waves. As we continue to uncover new information about Saturn and its rings, these findings will serve as a critical foundation for future research efforts aimed at further exploring the mysteries of our solar system.

7 Acknowledgement

I gratefully acknowledge the Maker of the Universe, for unending inspiration and momentum to continue in times of greatest need. I also appreciate Prof. Matthew Hedman for helpful comments and suggestions. Lastly, I acknowledge Prof. Datta Somantika for the degree of freedom to pursue a project in planetary seismology, using tools in Fourier transformations. This research has made use of data obtained from the recent Cassini Mission (2004-2017), as well as softwares from Python libraries.

References

- [1] Alberto Calderón. Intermediate spaces and interpolation, the complex method. *Studia Mathematica*, 24:113–190, 1964.

- [2] J. E. Colwell, P. D. Nicholson, M. S. Tiscareno, C. D. Murray, R. G. French, and E. A. Marouf. The Structure of Saturn's Rings. In Michele K. Dougherty, Larry W. Esposito, and Stamatios M. Krimigis, editors, *Saturn from Cassini-Huygens*, page 375. 2009.
- [3] Marie Farge. Wavelet transforms and their applications to turbulence. *Annual Review of Fluid Mechanics*, 24(1):395–458, 1992.
- [4] Richard G. French, Colleen A. McGhee-French, Philip D. Nicholson, and Mathew M. Hedman. Kronoseismology iii: Waves in saturn's inner c ring. *Icarus*, 319:599–626, 2019.
- [5] A. Grossmann and J. Morlet. Decomposition of hardy functions into square integrable wavelets of constant shape. *SIAM Journal on Mathematical Analysis*, 15:723–736, 07 1984.
- [6] M. M. Hedman and P. D. Nicholson. KRONOSEISMOLOGY: USING DENSITY WAVES IN SATURN's c RING TO PROBE THE PLANET's INTERIOR. *The Astronomical Journal*, 146(1):12, jun 2013.
- [7] M. M. Hedman and P. D. Nicholson. More Kronoseismology with Saturn's rings. , 444(2):1369–1388, October 2014.
- [8] M. M. Hedman, P. D. Nicholson, and R. G. French. Kronoseismology. IV. six previously unidentified waves in saturn's middle c ring. *The Astronomical Journal*, 157(1):18, dec 2018.
- [9] Christopher R. Mankovich. Saturn's Rings as a Seismograph to Probe Saturn's Internal Structure. *AGU Advances*, 1(2):e00142, June 2020.
- [10] Mark. S. Marley and Carolyn C. Porco. Planetary acoustic mode seismology: Saturn's rings. *Icarus*, 106:508–524, 1993.
- [11] A. Mertins. *Signal Analysis: Wavelets, Filter Banks, Time-Frequency Transforms and Applications*. Ultrasound in Biomedicine Research Series. Wiley, 1999.
- [12] Philip D. Nicholson, Maren Leyla Cooke, and Emily O. Pelton. An absolute radius scale for saturn's rings. *The Astronomical Journal*, 100:1339, 1990.
- [13] M.C. Pereyra and L.A. Ward. *Harmonic Analysis: From Fourier to Wavelets*. IAS/Park city mathematical subseries. American Mathematical Society, 2012.
- [14] Soumen Roy. Nonorthogonal wavelet transformation for reconstructing gravitational wave signals. *Physical Review Research*, 4(3), jul 2022.
- [15] Matthew S. Tiscareno, Joseph A. Burns, Philip D. Nicholson, Matthew M. Hedman, and Carolyn C. Porco. Cassini imaging of saturn's rings. *Icarus*, 189(1):14–34, jul 2007.
- [16] Christopher Torrence and Gilbert P. Compo. A practical guide to wavelet analysis. *Bulletin of the American Meteorological Society*, 79(1):61 – 78, 1998.